Journal of Chromatography, 480 (1989) 141–155
Elsevier Science Publishers B.V., Amsterdam — Printed in The Netherlands

CHROM. 21 694

HIGH-SENSITIVITY FLUORESCENCE DETECTOR FOR FLUORESCEIN ISOTHIOCYANATE DERIVATIVES OF AMINO ACIDS SEPARATED BY CAPILLARY ZONE ELECTROPHORESIS

SHAOLE WU and NORMAN J. DOVICHI*
Department of Chemistry, University of Alberta, Edmonton, Alberta T6G 2G2 (Canada)

SUMMARY

A fluorescence detector has been developed for capillary zone electrophoresis that produces a ten-fold improvement in precision compared with the previous state-of-the-art in fluorescence detection. This instrument, which is based on a sheath-flow cuvette flow chamber and a 0.05-W argon ion laser beam, combines a high numerical aperture collection optic, N.A. = 0.65, with a high quantum yield photomultiplier tube, $\Phi \approx 0.15$ at the wavelength of maximum emission. Detection limits (3σ) range from the injection of $1.7 \cdot 10^{-21}$ mol ($1.3 \cdot 10^{-12}$ *M*) of fluorescein isothiocyanate (FITC)-labeled arginine, the best case, to $6 \cdot 10^{-21}$ mol ($5.6 \cdot 10^{-12}$ *M*) of FITC-cysteine, the worst case. Signal linearity extends for at least five orders of magnitude from the detection limit to greater than 10^{-16} mol (10^{-7} *M*) injected.

INTRODUCTION

Capillary separation techniques offer remarkably high separation efficiencies for the analysis of complex mixtures[1]. Also, the small dimensions of the capillary tube offer substantial opportunities for the analysis of extremely small samples. Perhaps the most spectacular examples of microchemical analysis with capillary separation is the analysis of the composition of individual cells[2,3]. However, given the small amount of material availale for analysis, a high-sensitivity detector is often required for capillary separations.

A number of reviews have appeared on capillary zone electrophoresis[4–6]. High-sensitivity detectors used for capillary electrophoresis include those based on mass spectrometry[7], electrochemistry[3,8], laser-induced thermo-optical absorbance techniques[9] and laser-induced fluorescence[10]. Laser-induced fluorescence is particularly interesting because the detection sensitivity extends to near the single molecule level in favorable cases[11–13]. Recently, this group reported laser-induced fluorescence detection limits of the order of 10^{-20} mol for the capillary zone electrophoresis separation of amino acids labeled with fluorescein isothiocyanate[14]. It is desirable to lower these detection limits to the single molecule limit; counting the molecules of analyte within a sample represents the ultimate level of precision and quantitative analysis.

0021-9673/89/$03.50

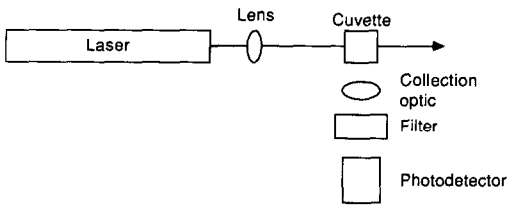

Fig. 1. Schematic diagram of a laser-induced fluorescence experiment. Light from a laser is focused with a lens into the sample cuvette. Fluorescence is collected at right-angles, filtered and detected with a photodetector.

In this paper, we describe several incremental improvements to the laser-induced fluorescence detector that result in roughly a factor of ten improvement in detection limit. To understand the high performance of the instrument, it is necessary to understand how the individual components of the instrument are combined to produce a high-efficiency detector.

OPTICAL DESIGN

A laser-induced fluorescence detector (Fig. 1) consists of a laser, a focusing lens, a sample cuvette, collection optics, a filter or monochromator and a photodetector. The design of the system is guided by two principles. First, the instrument should be simple and should use the minimum number of components. By reducing the component count and by simplifying the instrument design, the cost, reliability, stability and ease of use of the instrument will be improved. Second, the instrument should be designed to maximize the detection of photons generated by fluorescence while minimizing the background signal intensity. The fluorescence detector described in this paper approaches the ideal embodied in these principles.

Laser

At least three criteria are important in chosing the laser. First, the wavelength of the laser must match the absorbance spectrum of the analyte. In general, a compromise must be made in the choice of laser wavelength as different analytes present in a mixture will tend to have different absorbance spectra. However, if the same reagent is used to label all of the analyte, it is possible to optimize the laser wavelength. In particular, fluorescein isothiocyanate may be used as a derivatizing reagent for amino acids, peptides and proteins[15–21]. Amino acids derivatized with this molecule have an absorbance maximum at 490 nm, near the 488-nm line of the argon ion laser.

A more subtle point occurs in the choice of the laser wavelength. As it turns out, Raman scatter from the solvent is the major source of background signal in a well designed fluorescence detector. For water, there are two major Raman bands, one at about 1650 cm^{-1} and the other extending from 3100 to about 3700 cm^{-1}. There are also two minor Raman bands at 1640 and 2200 cm^{-1} (refs. 22–24). Ideally, the analyte will have a large Stokes shift so that the emission wavelength occurs at wavelengths that are much longer than the 3700 cm^{-1} band. Unfortunately, with fluorescein isothiocyanate and many other labels, the Stokes shift for emission is small. Instead, the excitation wavelength should be chosen so that the analyte emission wavelength

occurs between the two main Raman bands. The fluorescence emission of fluorescein-labeled amino acids maximizes at about 530 nm, where the Raman signal is relatively weak.

Spatial mode quality is a second criterion in choosing a laser. The beam must be focused to a small spot to excite efficiently the analyte eluted from the separation capillary. Continuous-wave gas lasers, such as the argon ion laser, possess high spatial coherence and may be focused to a few micrometers spot size. On the other hand, pulsed lasers tend to possess poor spatial quality and may be focused to a small spot only with difficulty.

Additional criteria are related to laser power and noise. To a first approximation, a high laser power is desirable. Both the fluorescence and background signals are expected to increase linearly with laser power. Under shot-noise conditions, the noise in the background increases with the square root of laser power; detection limits scale with the inverse square root of laser power. This shot-noise limit is the reason why lasers are employed in high-sensitivity fluorescence detectors. The high irradiance of a focused laser beam results in better detection limits than can be produced by an incoherent light source.

Although the high power of the laser is valuable in fluorescence measurements, the power and irradiance of the beam cannot be increased without bound. At high irradiance levels, optical saturation of the absorbance transition becomes significant. Under the saturation conditions, a significant fraction of the analyte is raised to the excited state. To a first approximation, saturation becomes important when the number of photons absorbed per second approaches the spontaneous emission rate. For highly fluorescence dye molecules, the laser irradiance should be held to a value less than 10^5 W cm^{-2} to eliminate saturation. In addition to saturation, molecules can undergo photodegradation under intense illumination. To minimize photodegradation, either a low-power beam must be employed or the illumination time of the molecule must be kept very short by using a high linear flow velocity.

Both saturation and photodegradation limit the utility of pulsed lasers for fluorescence excitation in capillary zone electrophoresis. Instead, modest power and inexpensive argon ion lasers may be employed in fluorescence detection. Even then, it is necessary not to focus the beam extremely tightly; a Gaussian 20-mW beam focused to a 1-μm radius spot size will produce a peak irradiance of over 10^6 W cm^{-2}.

A high-stability laser is required to obtain shot-noise limited performance. An argon ion laser, operating in the light regulated mode, will produce a short-term stability of about 0.1%. The laser is available with powers ranging from a few milliwatts to more than 10 W of power. A low-power argon ion laser is well suited for high-sensitivity fluorescence detection for capillary zone electrophoresis.

Focusing optics

It is appropriate to focus the laser beam to a spot that matches the size of the sample stream produced in the flow cell. For small-diameter capillary tubes, this sample stream must be of the order of tens of micrometers to minimize the detector volume. Inexpensive and high-quality microscope objectives may be used to focus the laser beam. These lenses are very well corrected for aberrations, are readily available and are very easily manipulated and exchanged for other optics.

Sample cuvette

To avoid extra-column band broadening, it appears necessary to perform fluorescence detection directly on-column in capillary zone electrophoresis. Given 10^6 theoretical plates, the allowed detector volume should be much less than 40 pl for a 50 cm × 10 μm I.D. column. Any plumbing associated with the transfer of the analyte to a detector cell would appear to introduce unacceptable band broadening. However, fluorescence detection using the capillary as the detection chamber is difficult. Light scatter generated at the air–column and column–sample interfaces results in large background signals in fluorescence detection. This scattered light can be reduced in several ways. First, an obscuration bar can be introduced in the plane perpendicular to the capillary surface to block much of the scattered light; unfortunately, much of the fluorescence will also be blocked by this bar[25]. Second, the capillary can be tilted with respect to the laser beam and the detection optics so that the scattered light is deflected away from the collection optics[26,27]. Third, the capillary can be tilted at Brewster's angle and a polarized laser beam can be used to that the scattered light originating at the air–column interface is extinguished[28]. Unfortunately, in each instance, it is necessary to image the fluorescence signal through the curved capillary wall; aberrations will inevitable degrade the fluorescence signal. Also, light scatter originating at the column–sample interface will contribute significantly to the background fluorescence signal.

Rather than detecting fluorescence directly on the capillary, it is possible to use the sheath-flow cuvette for fluorescence detection[11–14,25,26,29–32]. The capillary is introduced into a 250-μm square flow chamber constructed from good-optical quality quartz. A sheath stream, provided by a high-stability syringe pump, surrounds the sample stream at the exit of the capillary. At the very low flow-rates employed in electrophoresis, the flow profile is laminar. The sheath stream has the same composition as the separation buffer and is connected to electrical ground to complete the circuit for the electrophoresis. Because the sample and sheath have identical composition, no light scatter occurs at their interface, greatly reducing the background signal. The size of the sample stream is determined both by the relative volumetric flow-rates of the sample and sheath streams[33] and by diffusion of the analyte into the sheath stream[34]. A 1 m × 50 μm I.D. capillary operated at 25 kV will produce a sample stream diameter of 10 μm for a sheath stream flow-rate of 0.5 ml h^{-1}.

Collection optics

The fluorescence generated from the illuminated sample stream must be collected with high efficiency while scattered light reaching the detector must be minimized in order to obtain optimum detection limits. High numerical aperture microscope objectives may be used to collect fluorescence. The fraction of light collected by a lens is related to its numerical aperture, N.A., and the refractive index of the surrounding medium, n:

$$\text{collection efficiency} = \sin^2\left[\frac{\arcsin(\text{N.A.}/n)}{2}\right] \quad (1)$$

where a collection efficiency of 1 implies that the lens collects all of the photons emitted by the molecule. Usually, the lens is surrounded by air and $n = 1.0$. Table I lists the

TABLE I

COLLECTION EFFICIENCIES OF DIFFERENT LENSES (n = 1)

Numerical aperture	*Collection efficiency*	*Numerical aperture*	*Collection efficiency*
1.0	0.50	0.5	0.067
0.9	0.28	0.4	0.042
0.8	0.20	0.3	0.023
0.7	0.14	0.2	0.010
0.6	0.10	0.1	0.003

collection efficiency for lenses of different numerical aperture. Note that a lens of very high numerical aperture is required to obtain a high collection efficiency. A lens with a numerical aperture of 1 will collect half of the light emitted by the sample; although oil and water immersion lenses can have numerical apertures greater than 1, they collect less than 50% of the emitted light because the refractive index of the immersion fluid will be larger than the numerical aperture. An $f/1$ lens has a numerical aperture of about 0.5 and collects only 7% of the emitted light.

An interesting constraint exists in the choice of the lens. Fluorescence must be imaged from a *ca.* 10-μm^3 region in the center of the sheath flow cuvette. However, the cuvette is equipped with relatively thick windows, typically 2 mm, which requires the use of an objective with a working distance (the distance from the exit of the lens to the sample) of greater than 2 mm. Unfortunately, few lenses are designed with both high numerical aperture and long working distances. Expensive objectives with reasonable numerical aperture (0.65) are available with a working distance greater than 3 mm. These objectives are used in microelectronics inspection applications and work well for the detection of fluorescence emitted from an analyte within a sheath-flow cuvette.

A pinhole is placed in the image plane of the lens to isolate the illuminated sample region while rejecting light scattered from the cuvette walls. The size of the pinhole is matched to the size of the image of the illuminated region. A 10-μm radius sample stream would require a 600-μm diameter pinhole if a 30 × microscope objective were used as the collection optic.

Instead of a microscope objective, a high aspect ratio parabolic or hyperbolic mirror might be employed in the collection of the fluorescence signal[35]. Although these mirrors can collect over 50% of the emitted light, they suffer from a very high background signal. The mirrors produce poor image quality and, as a result, it is not possible to use a mask to block light scattered from the cuvette boundaries[36].

Spectral filters

If the appropriate laser wavelength has been chosen, the fluorescence will have a minimal spectral overlap with Raman and Raleigh scatter. Either a monochromator or a spectral filter may be used to isolate spectrally the fluorescence from the background scatter signal. The monochromator may be tuned to transmit a wavelength band that maximizes the signal-to-background ratio. Also, the bandwidth of the monochromator may be adjusted, within limits, by changing the size of the exit slit. Unfortunately, monochromators have limited transmission efficiency; an $f/4$ mono-

chromator will transmit roughly 0.3% of the incident intensity at the maximum of the transmission band. Also, our design criterion of simplicity argues against the use of monochromators in the detector.

On the other hand, spectral filters provide high transmission (>50%) and are very simple. In practice, it is necessary to use the filter to block both the Raleigh scattered light at the laser wavelength and the Stokes-shifted Raman scatter. We use a long-wavelength pass colored glass filter to block the Raleigh scatter; these filters are available with extremely high optical density at the laser wavelength, $T < 10^{-5}$, and high transmission at the maximum of the fluorescence band, $T = 90\%$. A short-wavelength pass interference filter is used to block the main Raman scatter band at 570 nm. The combination of the interference filter and the colored glass filter produces a band-pass filter optimized for the analysis of fluorescein isothiocyanate-labeled molecules. A subtle point concerns the orientation and location of the filters. The colored glass filter will fluoresce slightly when illuminated at the laser wavelength. By placing the interference filter after the glass filter, that portion of the fluorescence that is generated at wavelengths longer than 570 nm will be blocked. The filters should be placed either close to the microscope objective or immediately after the spatial mask. If the filters are close to the objective, only a small portion of the fluorescence will be emitted in a direction to pass through the limiting aperture and reach the photodetector. Similarly, by placing the filter after the spatial mask, the amount of scattered laser light that reaches the filter will be minimized.

Use of interference filters requires some care. The band-pass of the filter will change with the angle of incidence of light. To use the filters best, it is appropriate that they be placed in a collimated beam. The light from the microscope objective converges slowly and produces negligible deviation in spectral band-pass of the filter. Also, to obtain maximum performance of the filters, stray light must be reduced to an absolute minimum. We have a set of three baffles in the optical train to minimize light leaking into the photodetector. The inside of the light-tight optical system is coated with flat black paint to minimize any stray reflections that might reach the photodetector.

Future work may apply the recently commercialized Bragg diffraction filter that is based on diffraction of light from a regular three-dimensional array of polystyrene spheres[37]. These filters have very high extinction coefficient at the laser wavelength and may prove ideal for the rejection of Raleigh scatter.

Photodetector

It is necessary to convert the fluorescence signal into an electrical signal with high efficiency. Conventionally, a photomultiplier tube is used in this application. In the wavelength region near 550 nm, the maximum for analyte emission, both gallium arsenide and multi-alkali photocathodes provide quantum efficiencies greater than 10%. Although the gallium arsenide tubes produce slightly higher quantum efficiency, they are not ideal for fluorescence detection because of their limited dynamic range; modest intensity will damage the sensitive photocathode. Given the very high price of the gallium arsenide tubes, their fragility is a definite detriment to their use. Instead, we find that multi-alkali photomultiplier tubes produce good results. These tubes are relatively inexpensive, (*ca.* U.S.$ 380) and are fairly rugged. In the region near 550 nm, the Hamamatsu R1477 tube is useful. Although we do not know the quantum yield of the tube at 550 nm, the quantum yield at 450 nm is listed as 22%. We estimate the quantum yield of the tube to be about 15% at 550 nm.

It may be surprising to find that the photomultiplier tube dark count is not an important criterion for fluorescence applications. The high background count rate, which is inevitable in fluorescence measurements, will be much greater than the dark count of any photomultiplier tube.

On the other hand, the time response of the tube is important in photon counting and time-correlated photon counting. Those tubes which are based on a squirrel-cage dynode structure may be operated to produce a very fast temporal response. Using a published procedure for wiring the tube base, we obtain a rise-time of about 500 ps and a pulse width of 1.5 ns for the single photon response of the R1477 tube.

An interesting alternative photodetector has recently become available for photodetection in fluorescence measurements. A high-gain avalanche photodiode is available from RCA (Model C30902) that has single photon response and a detection quantum yield of greater than 35% at 550 nm. The diodes are small, with a 0.5 mm diameter active area. This small area would be useful in our application because the active area could act as the limiting aperture at the image plane of the objective. The small size of the photodetector would be useful in the design of a compact instrument. The main limitation of the photodiode is a limited count rate of $2 \cdot 10^6$ photons^{-1}; to use these photodiodes, it is necessary to minimize the background signal to low levels.

Construction

In the instrument, it is necessary to align a tightly focused laser beam with a small-diameter sample stream so that the fluorescence passes through a high numerical aperture objective that is fitted with a 600-μm limiting aperture. Designing the optical system so that the alignment may be optimized quickly is not a trivial task. In the current version of the instrument, we fix the location of the photomultiplier tube, the collection optic and the limiting aperture. All other components are aligned with respect to the collection optic. An auxiliary microscope is placed opposite the collection optic and used to assist the alignment of the cuvette. It is vital that the alignment microscope be fitted with a high-efficiency colored glass filter to block any scattered laser light to eliminate any ocular hazard.

A simple trick is used to align the remainder of the optical system. A small flashlight bulb may be placed after the pinhole but before the photomultiplier tube. When the light bulb is energized, light will travel back through the optical system in a path that is the reverse of fluorescence; the image of the pinhole is projected through the collection optic. The auxiliary microscope is focused on the light exiting the collection optic to produce a crisp image of the pinhole. The remaining optical elements are adjusted to superimpose the projected image of the pinhole with the fluorescence from the sample stream. When the images superimpose, the system is in alignment.

The sheath-flow cuvette, which is mounted on a three-axis translation stage, is moved so that the flow chamber, when viewed through the auxiliary microscope, is centered on the light leaving the collection optic. Two mirrors are used to center the laser beam roughly on the lens that is used to focus the laser beam. Last, the laser beam focusing lens, which also is mounted on a three-axis translation stage, is adjusted so that the laser beam is focused on the sample stream and the image of the fluorescence from the sample is exactly superimposed on the image of the spatial mask that is projected by the collection optic. It takes roughly 15 min to bring the system to alignment and the alignment is very stable.

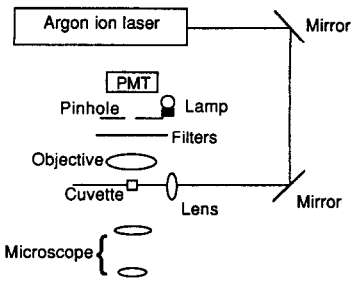

Fig. 2. Optical diagram. Light from a 488-nm argon ion laser is reflected from two mirrors and focused with a 2.5 × microscope objective into the center of a sheath-flow cuvette. Fluorescence is collected with a 0.65 N.A., 32 × microscope objective. The fluorescence is filtered and the illuminated sample is imaged on to a 600-μm diameter pinhole. The transmitted light is detected with a photomultiplier tube. An auxiliary microscope is used to inspect the sample stream and to assist in the alignment of the system. A small lamp is provided to illuminate the pinhole; in the alignment step, the image of the pinhole is superimposed with the fluorescence from the illuminated sample stream. A shutter and microswitch are used to prevent light from the lamp reaching the photomultiplier tube, preventing catastrophic damage to the tube if the lamp is illuminated while the photomultiplier tube is powered.

EXPERIMENTAL

Optics

The optical system (Fig. 2) was constructed on a 4 × 8 ft optical table, Model KST48 (Newport, Fountain Valley, CA, U.S.A.). A Model 99 argon ion laser (Innova, Mountain View, CA, U.S.A.) was operated in the light-regulated mode at a power of 0.05 W and a wavelength of 488 nm. The laser beam was reflected from two front-surface coated mirrors and focused with a 2.5 ×, 45 mm focal length microscope objective (Melles Griot, Irvine, CA, U.S.A.) into the sheath-flow cuvette. The cuvette, Model 300-0511-000 (Ortho Diagnostics, Westwood, MA, U.S.A.), has a 250-μm square flow chamber with 1.5-mm thick quartz windows. Unfortunately, the manufacturer of our sheath-flow cuvette has ceased production of this item. Coulter (Hialeah, FL, U.S.A.) and Becton-Dickinson (Mountain View, CA, U.S.A.) also produce these cuvettes; we have had no experience with their products. Fluorescence from the sample was collected with a 32 ×, 0.60 N.A. microscope objective, Model 2569-1130 (Leitz/Wild, Calgary, Canada) and imaged on to a 0.6 mm diameter pinhole. A colored glass filter, Model OG 515 (Schott Glass Technologies, Duryea, PA, U.S.A.), and an interference filter, Model 35-5347 (Ealing Saint-Laurent, Quebec, Canada), were used to block scattered light. A photomultiplier tube, Model R1477 (Hamamatsu, San Jose, CA, U.S.A.), wired for a fast response[38], was used to detect fluorescence. The photomultiplier tube was operated at 1000 V with a Model 204 photomultiplier power supply (Pacific Precision Instruments, Concord, CA, U.S.A.). The output of the photomultiplier tube was conditioned with a 40-kΩ resistor and a 5-μF capacitor to produce a 0.4-s detector time constant. The resulting voltage was displayed on a strip-chart recorder.

Electrophoresis

The electrophoresis capillary is 1 m × 50 μm I.D. × 180 μm O.D. fused silica

(Polymicro Technology, Phoenix, AZ, U.S.A.). The tubing is inserted into the sheath-flow cuvette and held in place with a locally machined ferrule system. A 30-kV power supply, Model RHR120W (Spellman, Plainview, NY, U.S.A.) is used to drive the electrophoresis. The high-voltage end of the capillary is enclosed within a safety interlock-equipped Plexiglas box. The sheath fluid is provided by a high-pressure syringe pump, Model 314 (Isco, Lincoln, NE, U.S.A.). Samples were injected by shutting off the sheath-flow pump and using electromigration at 1 kV for 10 s. Samples and the separation buffer were held in 500-μl plastic disposable centrifuge tubes.

Reagents

Fluorescein isothiocyanate (FITC), isomer I and the amino acids were obtained from Sigma (St. Louis, MO, U.S.A.). The separation buffer was a pH 10, 50 m*M* aqueous carbonate buffer. FITC-labeled amino acids were prepared as before[14].

RESULTS

The separation of a mixture of six FITC-labeled amino acids is shown in Fig. 3. Except for cysteine, all of the amino acids produce a single peak in the separation. Cysteine produces two peaks, presumably because of multiple labeling of the compound. These six amino acids are well separated except for one cysteine peak that overlaps alanine. Note that the reagent peaks, which elute between 9.5 and 10.5 min, are much lower in amplitude than in our previous work[14]. Consistent treatment of all of the amino acids helps to decrease greatly the reagent background. The theoretical plate count is about 400 000 for the amino acids, although lysine exhibits some tailing and a slightly poor plate count.

Calibration graphs for the amino acids were constructed from 10^{-10} to 10^{-7}

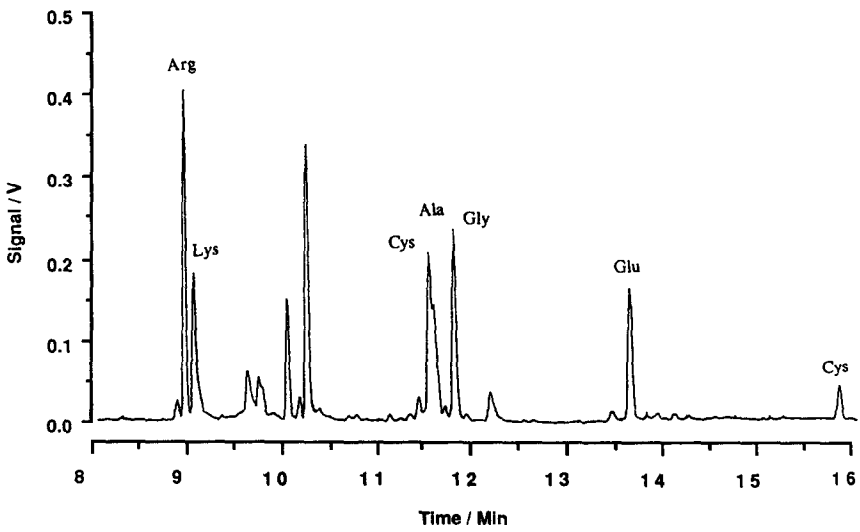

Fig. 3. Separation of FITC-labeled amino acids. The concentrations of arginine, lysine, alanine, glycine and glutamic acid were $1.14 \cdot 10^{-9}$ *M* and that of cysteine was $3.42 \cdot 10^{-9}$ *M*.

TABLE II

DETECTION LIMITS

Amino acid	*Injection volume (nl)*	*Detection limit*[a]		
		Concentration (10^{-2} M)	*Amount (10^{-21} mol)*	*Molecules*
Alanine	1.1	3.0	3.0	1900
Arginine	1.3	1.3	1.7	1100
Cysteine	1.1	5.6	5.9	3600
Glutamic acid	0.9	3.0	2.7	1600
Glycine	1.1	1.9	2.0	1200
Lysine	1.3	2.1	2.8	1700

[a] Detection limits refer to the amount of analyte injected into the capillary that produces a signal that is three times larger than the standard deviation of the background signal.

M for FITC-labeled arginine, glycine, glutamic acid, lysine and alanine and from $5 \cdot 10^{-10}$ to $5 \cdot 10^{-7}$ *M* for FITC-labeled cysteine. In all instances the calibration graphs were linear; the slope of the least-squares regression line through the plot of logarithm of signal *versus* logarithm of concentration was 1.00 with correlation coefficient of 1.00.

Detection limits (3σ) were calculated by recording 100 values of the signal at 1-s intervals and calculating the standard deviation of the background signal. This value was multiplied by 3 and divided by the slope of the calibration graphs. The 1-s sampling interval is appropriate for this experiment because the peaks have a half-width (one standard deviation) of about 1 s. Further, the 0.2-s time constant of the electronics ensures that successive samples taken as 1-s intervals are not correlated. The detection limits for the six amino acids are listed in Table II. In the best case, with arginine, the detection limit corresponds to the injection of about 1 nl of $1.3 \cdot 10^{-12}$ *M* analyte or $1.7 \cdot 10^{-21}$ mol or 1000 molecules. The worst case is cysteine, with detection limits corresponding to an injected concentration of $6 \cdot 10^{-12}$ *M* or $6 \cdot 10^{-21}$ mol or 4000 molecules of analyte.

DISCUSSION

Background signal

The background signal observed in our instrument is 0.005 V developed across a 40-kΩ resistor, corresponding to a background current of 125 nA. This current is due solely to scattered laser light striking the photomultiplier tube; the dark current is several orders of magnitude lower. A high-speed sampling oscilloscope was used to measure the single photon response of the photomultiplier tube. For each photon detected, the tube produced a pulse of electrons containing $9 \cdot 10^{-13}$ C of charge, equivalent to a current amplification of $5.6 \cdot 10^{6}$. Given this current amplification, the 125-nA background signal is equivalent to the detection of $1.4 \cdot 10^{5}$ photons^{-1}. Over the 0.2-s time constant of the electronics, about $3 \cdot 10^{4}$ photons would be detected. The shot-noise in this photon count is 170 photons. The expected relative precision of the measurement would be 0.6%. The observed relative precision of the measurement,

determined from 100 data points taken at 1-s intervals, is 0.8%. The signal appears to be shot-noise limited.

It is commonly assumed that Raman scatter is the major source of background signal in laser-induced fluorescence measurements. Moskovits and Michaelian[23] presented data for two weak Raman bands, one due to the bending mode at 1640 cm^{-1} and an unassigned band at 2200 cm^{-1}. The combined intensity of these two bands has an integrated intensity that is about 1/70 times the intensity of the integrated O–H stretching bands at 3500 cm^{-1}. Using the data of Kondilenko *et al.*[24] for the integrated intensity of the 3500 cm^{-1} band, 10^{-29} cm^{-2} sr^{-1}, the intensity of the Raman bands that overlap the transmission spectrum of the filter pair is about $1.4 \cdot 10^{-31}$ cm^{-2} sr^{-1} $molecule^{-1}$ (ref. 24). There are 4π sr in the emission sphere so that the scatter intensity over all space is $2 \cdot 10^{-30}$ cm^2 $molecule^{-1}$. The excitation volume of $6 \cdot 10^{-12}$ l contains about $2 \cdot 10^{14}$ water molecules; the light scatter cross-section due to all of the water molecules is *ca.* $4 \cdot 10^{-16}$ cm^2. The irradiance of the 0.05-W laser beam, focused to a spot size, ω, of 10 μm, at 488 nm is given by

$$I = \frac{0.05 \text{ W}}{\pi(10\ \mu\text{m})^2} = \frac{0.05 \text{ W} \cdot 2.5 \cdot 10^{18} \text{ photons s}^{-1} \text{ W}^{-1}}{3 \cdot 10^{-6} \text{ cm}^2} = 4 \cdot 10^{22} \text{ photons cm}^{-2} \text{ s}^{-1} \qquad (2)$$

and the average number of photons scattered by the solvent is $I\sigma \approx 1.5 \cdot 10^7$ $photons^{-1}$. With a collection efficiency of 12%, a filter transmission function of 50% and a photomultiplier quantum yield of 15%, the Raman bands are expected to produce $1.4 \cdot 10^5$ $photons^{-1}$, equal to the observed background signal. It appears that the background signal is due, in part, to Raman scatter at the 140 and 2200 cm^{-1} bands.

Noise

The noise in the background signal was equal to a standard deviation of 170 photons averaged by a 0.2-s time constant. The detection limit corresponds to a signal that is three times larger than the noise in the background signal, or 510 photons emitted in a 0.2-s time period. The full width at half-maximum of the typical electrophoretic peak is about 3 s, corresponding to the emission of 7600 photons per peak. If the detection limit is 1100 molecules, then the average molecule will, while illuminated by the laser beam, emit seven photons that are detected by our photomultiplier tube. Assuming a 12% collection efficiency, 25% filter transmission function 15% photomultiplier quantum yield and 100% fluorescence quantum yield, the average molecule will cycle about 1500 times from the ground state to the excited state during passage through the laser beam. That is, the molecule appears to be absorbing, and emitting, an average of 1500 photons during its transition through the laser beam.

The detection limits produced by the improved instrument are, on average, a factor of ten superior to our previously reported results. These improved results arise from three sources. First, the improved instrument uses a photomultiplier tube with a three times higher quantum yield compared with the earlier instrument. Second, the improved instrument uses a microscope objective with a three times higher collection efficiency. These two improvements yield a ten-fold higher signal and, assuming shot noise, a three-fold improvement in precision.

The last improvement is rather subtle —the laser power was decreased by a factor of twenty to produce a factor of four improvement in signal-to-noise ratio. By decreasing the laser power from 1 W to 50 mW, the background signal was reduced by a factor of twenty. That is, the background signal changes linearly with laser power; assuming shot noise-limited measurement, the decrease in laser power would produce a four-fold decrease in the absolute noise. If one assumed a linear relationship between laser power and signal intensity, the decrease in laser power should have produced a twenty-fold decrease in fluorescence intensity, resulting in a net degradation in detection limit. However, the observed fluorescence intensity was, within experimental error, independent of laser power over the range studied.

Photodegradation

Both saturation and photodegradation of the analyte molecule could produce a fluorescence signal that is independent of laser power. Saturation is not particularly important in this instrument—the laser irradiance at the center of the beam is about a factor of ten lower than that value required to produce appreciable saturation. However, photodegradation of the molecule is important in our experimental system. Hirschfeld[39] demonstrated that fluorescein isothiocyanate can cycle from the ground state to the excited state about 7800 times before photodegrading. Because no increase in fluorescence occurs for an increase in laser irradiance above that required to photodegrade the analyte, our fluorescence signal is constant down to 0.05 W.

The irradiance profile of the Gaussian laser beam is given by

$$I(x,y) = \frac{2P}{\pi\,\omega^2} \cdot \exp\,(-2x^2/\omega^2) \cdot \exp\,(-2y^2/\omega^2) \tag{3}$$

where the sample flow is along the x direction. If the analyte molecule travels at the center of the beam, then $y = 0$ and

$$I(x,0) = \frac{2P}{\pi\,\omega^2} \cdot \exp\,(-2x^2/\omega^2) \tag{4}$$

The molecule is traveling at a constant linear velocity through the beam. The average linear flow-rate is given by the volumetric-flow rate, 0.5 ml^{-1}, divided by the cross-sectional area of the flow chamber, 250 μm^2. If the flow profile is parabolic and if the molecule travels at the center of the tube, the linear velocity of the analyte, v, is 16/9 times the average linear linear flow velocity, $v = 0.4\ cm^{-1}$ (ref. 40). The time-dependent irradiance observed by the analyte is then given by the position divided by the velocity of the molecule:

$$I(t) = \frac{2P}{\pi\,\omega^2} \cdot \exp\,[-2\,(x/v)^2/(\omega/v)^2] = \frac{2P}{\pi\,\omega^2} \cdot \exp\,[-2t^2/(\omega/v)^2] \tag{5}$$

Last, the total number of photons emitted by a molecule traveling through the beam is given by the integral over all time of the rate of photons emitted by the molecule:

$$N = \int_{-\infty}^{\infty} I(t)\,\sigma\,dt = \frac{2P\sigma}{\sqrt{2\pi\omega v}} = \frac{2 \cdot 1.2 \cdot 10^{17}\ \text{photons}^{-1} \cdot 1.8 \cdot 10^{-16}\ \text{cm}^2}{\sqrt{2\,\pi} \cdot 10^{-3}\ \text{cm} \cdot 0.4\ \text{cm}^{-1}}$$

$$= 4 \cdot 10^4\ \text{photons molecule}^{-1}. \quad (6)$$

This count of photons per molecule is the maximum expected because most molecules will not pass through the center of the laser beam but instead will be distributed over the sample stream area. However, the predicted count rate is about five times higher than the value estimated by Hirschfeld[39] for photodegradation.

Even given photodegradation of the fluorescein molecule, there is a factor of 5 difference in the observed (1500 photons molecule^{-1}) and predicted (7800 photons molecule^{-1}) fluorescence intensity. This different is explained by reagent purity (about 80%), completion of reaction, loss of very low concentration analyte on glassware and the capillary tubing, analyte not passing through the illumination region, reflective losses in the optical train, imperfect alignment of the system, fluorescence quantum yield less than 1 and degraded performance of the collection optic when imaging through the thick windows of the cuvette.

CHEMICAL CONTAMINATION

The purpose of this paper is to describe improvements to a high-sensitivity fluorescence detector for capillary electrophoresis. It is not intended to describe amino acid analysis at the detection limit of the instrument. In our experiment, samples of FITC-labeled amino acids were prepared at a concentration of less than 10^{-6} M; samples were prepared by serial dilution to generate material for analysis at concentrations near the detection limit. To label samples at the 10^{-12} M level will require significant attention to the cleanliness of the system. A 1-ml sample that is 10^{-12} M in amino acid will contain less than 1 pg of amino acid. Atmospheric contamination of samples due to dust particles would be virtually impossible to avoid at this very low concentration level. Instead, it probably will be necessary to resort to a flow system to prepare the derivatized amino acids.

There are two sources of background contamination in Fig. 3. The peaks in the region from 9.5 to 10.5 min are associated with the reagent blank. The remaining peaks are associated with impurities in the amino acids or are degradation products of the FITC-labeled amino acids.

FUTURE DIRECTIONS

Improvements in detection limit can be made either by increasing the fluorescence signal or by decreasing the noise in the background signal. The former approach appears to offer limited reward—the laser irradiance is sufficient to photodegrade the fluorescence signal. Also, the collection efficiency and photomultiplier quantum yield are both within a factor of two of the best that can be obtained. Instead, improvements in detection limit are to be found by decreasing the noise in the background signal. First, even lower power lasers must be employed in the

instrument; however, the low laser irradiance makes visual alignment of the system tedious. Next, given a shot-noise limited background signal, decreasing the noise in the background signal is to be achieved by decreasing the background signal. Improved spectral filters, particularly with better blocking filters at the excitation wavelength, should provide improved performance.

Pulsed laser excitation and time-gated detection offer an interesting, albeit non-trivial, approach to minimizing the background signal[41]. In this approach, a mode-locked argon ion laser is used to excite the analyte. Both light scatter and fluorescence are generated by the laser pulse. However, light scatter is a nearly instantaneous process whereas fluorescence is characterized by an exponential decay with a 3–5 ns lifetime. Fast electronics may be used to produce a fast anti-coincidence counter that only registers photoelectron events that are not coincident with the laser pulse. Although the 488-nm line of the laser is not commonly mode-locked, we have demonstrated that pulses of < 500 ps duration can be produced by the laser. With this instrumentation, it should be possible to reduce the background signal by two to four orders of magnitude while not perturbing the fluorescence signal. As a result, detection limits of a few analyte molecles may be obtained.

ACKNOWLEDGEMENTS

This work was funded by the National Sciences and Engineering Research Council through operating grant number A1482 and equipment grant number EQ E0321. Joel Harris of the University of Utah kindly supplied the base and socket for the photomultiplier tube.

REFERENCES

1 M. Novotny, *Anal. Chem.*, 53 (1981) 1294A.
2 R. T. Kennedy, R. L. St. Claire, III, J. G. White and J. W. Jorgenson, *Mikrochim. Acta*, II (1987) 37.
3 R. A. Wallingford and A. G. Ewing, *Anal. Chem.*, 60 (1988) 1973.
4 J. W. Jorgenson and K. D. Lukacs, *Science (Washington D.C.)*, 222 (1983) 266.
5 M. J. Gordon, X. Huang, S. L. Pentoney, Jr. and R. N. Zare, *Science (Washington, D.C.)*, 242 (1988) 224.
6 A. G. Ewing, R. A. Wallingford and T. M. Olefirowicz, *Anal. Chem.*, 61 (1989) 292A.
7 R. D. Smith, J. A. Olivares, N. T. Nguyen and H. R. Udseth, *Anal. Chem.*, 60 (1988) 436.
8 L. A. Knecht, E. J. Guthrie and J. W. Jorgenson, *Anal. Chem.*, 56 (1984) 479.
9 M. Yu and N. J. Dovichi, *Anal. Chem.*, 61 (1989) 37.
10 E. Gassmann, J. E. Kuo and R. N. Zare, *Science (Washington, D.C.)*, 230 (1985) 813.
11 N. J. Dovichi, J. C. Martin, J. H. Jett and R. A. Keller, *Science (Washington, D.C.)*, 219 (1983) 845.
12 N. J. Dovichi, J. C. Martin, J. H. Jett, M. Trkula and R. A. Keller, *Anal. Chem.*, 56 (1984) 348.
13 D. C. Nguyen, R. A. Keller, J. H. Jett and J. C. Martin, *Anal. Chem.*, 59 (1987) 2158.
14 Y. F. Cheng and N. J. Dovichi, *Science (Washington, D.C.)*, 242 (1988) 562.
15 H. Maeda, N. Isida, H. Kawauchi and K. Tuzimura, *J. Biochem.*, 65 (1969) 777.
16 K. Muramoto, H. Kawauchi, Y. Yamamoto and K. Tuzimura, *Agric. Biol. Chem.*, 40 (1976) 815.
17 K. Muramoto, H. Kawauchi and K. Tuzimura, *Agric. Biol. Chem.*, 42 (1978) 1559.
18 I. Simpson, *Anal. Biochem.*, 89 (1978) 304.
19 K. Muramoto, H. Kamiya and H. Kawauchi, *Anal. Biochem.*, 141 (1984) 446.
20 H. Kawauchi and K. Tuzimura, *Agric. Biol. Chem.*, 35 (1971) 150.
21 H. Kawauchi, K. Tuzimura, H. Maeda and N. Ishida, *J. Biochem.*, 66 (1969) 783.
22 G. E. Walrafen and L. A. Blatz, *J. Chem. Phys.*, 59 (1973) 2646.
23 M. Moskovits and K. H. Michaelian, *J. Chem. Phys.*, 69 (1978) 2306.

24 I. I. Kondilenko, P. A. Korotkov, V. A. Klimenko and O. P. Demyanenko, *Opt. Spectrosc. (USSR)*, 43 (1987) 384.
25 L. A. Herzenberg, R. G. Sweet and L. A. Herzenberg, *Sc. Am.*, 234 (1976) 108.
26 W. A. Bonner, H. R. Hulett, R. G. Sweet and L. A. Herzenberg, *Rev. Sci. Instrum.*, 43 (1972) 404.
27 S. Folestad, L. Johnson, B. Josefsson and B. Galle, *Anal. Chem.*, 54 (1979) 925.
28 W. G. Kuhr and E. S. Yeung, *Anal. Chem.*, 60 (1988) 1832.
29 M. R. Melamed, P. F. Mullaney and M. L. Mendelsohn, *Flow Cytometry and Sorting*, Wiley, New York, 1979.
30 D. Pinkel, *Anal. Chem.*, 54 (1982) 503A.
31 L. W. Hershberger, J. B. Callis and G. D. Christian, *Anal. Chem.*, 51 (1979) 1444.
32 T. A. Kelly and G. D. Christian, *Anal. Chem.*, 53 (1981) 2110.
33 F. Zarrin and N. J. Dovichi, *Anal. Chem.*, 57 (1985) 2690.
34 Y. F. Cheng and N. J. Dovichi, unpublished results.
35 M. J. Skogen-Hagenson, G. C. Saltzman, P. F. Mullaney and W. H. Brockman, *J. Histochem. Cytochem.*, 25 (1977) 784.
36 N. K. Seitzinger and R. A. Keller, paper presented at the *41st ACS Summer Symposium on Analytical Chemistry, Stanford University, June 26th, 1988.*
37 R. J. Carlson and S. A. Asher, *Appl. Spectrosc.*, 38 (1984) 297.
38 J. M. Harris, F. E. Lytle and T. C. McCain, *Anal. Chem.*, 48 (1976) 2095.
39 T. Hirschfeld, *Appl. Opt.*, 15 (1976) 3135.
40 R. B. Bird, W. E. Stewart, E. N. Lightfoot and T. W. Chapman, *Lectures in Transport Phenomena*, Americal Institute of Chemical Engineers, New York, 1969.
41 G. R. Haugen and F. E. Lytle, *Anal. Chem.*, 53 (1981) 1554.